Journal of Cleaner Production 328 (2021) 129645

Contents lists available at ScienceDirect

Journal of Cleaner Production

journal homepage: www.elsevier.com/locate/jclepro

Selective precipitation of calcium ion from seawater desalination reverse osmosis brine

Raffaele Molinari [a,*], Ahmet Halil Avci [a], Pietro Argurio [a], Efrem Curcio [a], Sandra Meca [b], Mireia Plà-Castellana [b], Jose Luis Cortina [c]

[a] Department of Environmental Engineering (DIAm), University of Calabria, Via P. Bucci, Cubo 44/A, Rende (CS), Italy
[b] Sustainability Area, EURECAT, Centre tecnològic de Catalunya, Spain
[c] Chemical Eng Dept, Barcelona TECH UPC, Spain

ARTICLE INFO

Handling editor: M.T. Moreira

Keywords:
Selective calcium precipitation
Seawater desalination reverse osmosis brine valorisation
Inhibition calcium precipitation by magnesium
Aragonite
Calcium precipitation by medusa equilibrium code
Calcium precipitation by PhreeqC modelling

ABSTRACT

The near zero liquid discharge (NZLD) approach, by recovering water and dissolved valuable salts, is the most attractive clean solution for the valorisation of brines from seawater desalination reverse osmosis (SWD-RO) plants. In this perspective, a key aspect is calcium removal/recovery, to avoid scaling problems in the successive advanced separation units for recovering other valuable salts. In this work sodium citrate ($Na_3C_6H_5O_7$), carbonate (Na_2CO_3) and hydrogencarbonate ($NaHCO_3$) were tested as calcium precipitation reagents. Different pH, temperature, ionic strength and reagent molar ratio were tested to maximize the Ca^{2+} precipitation and minimize the Mg^{2+} loss. Aqueous solutions containing Ca and Mg ions with/without all major seawater electrolytes were used. The chemical basis of the precipitation processes were discussed based on the effective ion surface density (e.g. Slater rule), ion hydration and Eigen association process of the precipitate formation in the complex multicomponent brine. PhreeqC and Medusa equilibrium numerical codes were applied on some experimental data of the precipitation processes providing a good agreement between calculated and experimental values. Ca^{2+} removal efficiency higher than 90% coupled with an Mg^{2+} loss below 7% was obtained at 60 °C and controlled pH, by using $NaHCO_3$. These results are very promising in view of designing a process for brines valorisation, thus mitigating the environmental problems related to SWD-RO brines disposal.

1. Introduction

Raw materials are vital for economic growth and competitiveness: securing reliable, sustainable and undistorted access to them is of strategic relevance to strengthen a long-term industrial leadership. Since 2011, the European Commission established and periodically upgraded a list of critical raw materials (CRM) on the basis of their high economic importance and high supply risk (European Commission, 2020). Research activities on innovative mining and recycling processes have been encouraged coherently with the paradigm of Circular Economy. In this respect, seawater – composed by 3.3% of dissolved salts - is a potentially unlimited source of minerals: it is estimated that sea and oceans store about $5{\cdot}10^{16}$ tons of minerals, with presence of almost all elements of the periodic table, although at ppm/ppb levels (Mero, 1965). In particular, the extraction of minerals from hypersaline brines generated as by-product of seawater desalination plants has attracted the interest of scientists: today, about 18,200 desalination plants operated worldwide with a global cumulative capacity near 90 million m^3/day (International Desalination Association,). This capacity is expected to grow at an increasingly rapid pace in the near future because of water shortage crisis around the world and increasing water demand (Badruzzaman et al., 2019). The treatment or disposal of concentrated brine is a major challenge of seawater desalination reverse osmosis (SWD-RO) processes, because discharging the brine back into the sea seriously affects the marine ecosystem and incurs additional costs to plants (Choi et al., 2018). Brine is a complex mixture containing high concentration of electrolytes (most abundant are Na^+, Mg^{2+}, Ca^{2+}, K^+ and Sr^{2+} among cations, Cl^-, SO_4^{2-}, Br^- among anions). Their selective extraction was attempted by different methodological approaches (Loganathan et al., 2017), including membrane technology such as forward osmosis (FO), pressure retarded osmosis (PRO), and membrane distillation (MD), to recover valuable resources or energy from the brine

* Corresponding author. Department of Environmental Engineering (DIAm), University of Calabria, via P. Bucci, Cubo 44/A, I-87036, Arcavacata di Rende (CS), Italy.
E-mail address: raffaele.molinari@unical.it (R. Molinari).

https://doi.org/10.1016/j.jclepro.2021.129645
Received 7 July 2021; Received in revised form 1 October 2021; Accepted 6 November 2021
Available online 9 November 2021

while producing water (Bouchrit et al., 2015; Martinetti et al., 2009). When implementing a technological platform for brine pre-concentration and subsequent extraction of valuable minerals, the removal of calcium is usually recognized as a priority in upstream section. This is due to the critical inorganic fouling issue – properly referred to as "scaling" - related to the precipitation of sparingly Ca-soluble salts such as $CaCO_3$(s) and $CaSO_4$ $2H_2O$ (Antony et al., 2011; Quist-Jensen et al., 2016; Giwa et al., 2017).

Some papers in the scientific literature are dedicated to the specific problem of calcium removal from seawater desalination brines and are described in the following. Reactive precipitation tests, carried out on seawater nanofiltration retentate with $NaHCO_3$/Na_2CO_3 resulted in a reduction of Ca^{2+} ions of 56 and 89% for initial pH values of 9 and 9.9, respectively; in addition, incorporation of $MgCO_3$ in the overgrowths with extent between 8 and 10 mol % was observed (Drioli et al., 2004). Sorour et al. (2015) proposed a combined precipitation/chelation process for selective separation of Ca and Mg from SWD-RO brine; first stage of reactive precipitation by Na_2CO_3 at pH 9.2 resulted in a 93.2% Ca removal as $CaCO_3$(s), while second stage of reactive precipitation by NaOH at pH 12 led to 74% Mg recovery as $Mg(OH)_2$(s). The decalcified filtrate of the second precipitation stage was further processed for almost complete removal of Mg using EGTA, DTPA and HEDTA as chelating compounds (Sorour et al., 2016).

According to Natasha and Lalasari (2017), precipitation tests with oxalic acid on desalination brine (total dissolved salts ~96 g/L) resulted, in the best condition (40 ml of $C_2H_2O_4$ (100 g/L) added to 50 ml of brine), in about 98% calcium removal. Bubbling CO_2(g) into SWD-RO brine from an initial pH of 10.5 until reaching a final value of 8, Bang et al. (2017) observed a decrease of Ca^{2+} concentration from 714 to tens of mg/L (prevalently precipitated as calcite), while Mg^{2+} concentration was reduced by about 20%; this procedure, cycled five times, finally led to 86% precipitation of hydromagnesite. This approach is very promising in terms of environmental sustainability, giving the possibility of achieving fixation of CO_2(g) using Ca^{+2} and Mg^{+2} ions. On this aspect, Wang et al. (2011) evidenced that by adequately adjusting pH and CO_2 partial pressure it is possible to precipitate over 90% of the Ca^{2+} and Mg^{2+} ions contained in seawater in the forms of $MgCO_3$ and dolomite [$MgCa(CO_3)_{2(s)}$] with an acceptable process kinetics. Since each m^3 of natural seawater could fix about 2.65 kg of CO_2, and that the potential of concentrated seawater is 2–3 times this value, it can be observed that even if the annual CO_2 emissions of the entire world were captured in this way, the concentration of Ca and Mg ions in natural seawater would change at only the part-per-million scale, giving a negligible ecological effect.

An important aspect to be considered when removing calcium from SWD-RO brine is process selectivity. In particular, the Mg^{2+} ion has an important effect on the scale formation in terms of kinetics, morphology, and Mg/Ca ratio in the precipitate. It was evidenced that the Mg^{2+} ion adsorbs onto the deposited crystals and the ratio of Mg^{2+} in the precipitate is proportional to the ratio of Mg/Ca in the scaling water (Chen et al., 2006). This trend was previously observed by Zhang and Dawe (2000). Their results showed that the calcite growth rate is reduced by the presence of Mg^{2+}, and it decreased by increasing Mg/Ca ratio in the supersaturated solution. The authors proposed that Mg^{2+}, being incorporated into the original calcite seed surfaces, inhibited calcite growth by developing new crystal surfaces. Besides, in the case of $CaSO_4$ crystal formation and precipitation, it was also found that the presence of Mg^{2+} reduced the Ca^{2+} removal efficiency because of the stronger electronegativity of Mg^{2+} when compared to that of Ca^{2+} (Choi et al., 2018).

In pursuing the strategy of valorising desalination waste, further investigations are necessary in order to fill the knowledge gap existing in the scientific literature. In this work, sodium citrate ($Na_3C_6H_5O_7$), sodium carbonate (Na_2CO_3) and sodium bicarbonate ($NaHCO_3$) were tested as precipitant agents for the selective removal of calcium from SWD-RO brines. With the aim to reduce the loss of magnesium due to co-precipitation (the second most abundant cation in seawater), experiments were carried out at different pH, temperature, ionic strength and reagent molar ratio. Chemical speciation of Ca and Mg precipitation, by using PhreqC-Pitzer and Medusa equilibrium calculation tools, has been carried out and correlated with the experimental data. Overall, these novel results contribute to the development of a sequential approach for the extraction of salts dissolved in rejected brine.

2. Theoretical aspects on Ca(II)/Mg(II) precipitation in SWRO brines

Reduction of the Ca(II) content from SWD-RO brines was postulated by using two routes with two different precipitating anions: i) citrate ($C_6H_5O_7^{3-}$, Cit^{3-}) and ii) carbonate by using Na-Citrate, $NaHCO_3$ and Na_2CO_3 solutions respectively. Various parameters as pH, temperature, ionic strength and reagent molar ratio on the Ca and Mg selective precipitation, were theoretically studied preliminarily. SWD-RO brine is a complex mixture of many strong electrolytes with concentration values of the main ions between 10^{-3}–1 M. Considering the unitary activity coefficients, the activity becomes equal to molality but this one can be substituted by the molar concentration. Indeed, for the synthetic brine composition used in this work (foreseen density 1.050–1.060 kg/L), the calculated molalities were a little higher than the corresponding molar values with the highest value within +2%, thus brine can be considered a low concentrated solution and the molar concentrations (mol/L solution) will be considered along the work.

2.1. pH dependence of Ca(II) and Mg(II) precipitation with citrate and carbonate ions

The pH plays an important role, as it can be seen in the following, summarizing the more relevant species affecting the Ca(II) and Mg(II) precipitation reactions and the equilibrium constants associated (omitting H_2O and H_3O^+ for simplicity) at 298 K:

$$H_3Cit \leftrightarrows H_2Cit^- + H^+ \quad \log K_{c1} = -3.13 \tag{1}$$

$$H_2Cit^- \leftrightarrows HCit^{2-} + H^+ \quad \log K_{c2} = -4.76 \tag{2}$$

$$HCit^{2-} \leftrightarrows Cit^{3-} + H^+ \quad \log K_{c3} = -6.40 \tag{3}$$

$$H_2CO_3 \leftrightarrows HCO_3^- + H^+ \quad \log K_{a1} = -6.35 \tag{4}$$

$$HCO_3^- \leftrightarrows CO_3^{2-} + H^+ \quad \log K_{a2} = -10.33 \tag{5}$$

Both anions Cit^{3-} and CO_3^{2-} are forming Ca(II) and Mg(II) complexes according to reactions (6) to (15):

$$Ca^{2+} + CO_3^{2-} \leftrightarrows CaCO_3(aq) \quad \log K_1 = -7.1 \tag{6}$$

$$Mg^{2+} + CO_3^{2-} \leftrightarrows MgCO_3(aq) \quad \log K_2 = -7.4 \tag{7}$$

$$Ca^{2+} + HCO_3^- \leftrightarrows CaHCO_3^+ \quad \log K_3 = 1.1 \tag{8}$$

$$Mg^{2+} + HCO_3^- \leftrightarrows MgHCO_3^+ \quad \log K_4 = 1.1 \tag{9}$$

$$Ca^{2+} + Cit^{3-} \leftrightarrows CaCit^- \quad \log K_5 = 4.87 \tag{10}$$

$$Ca^{2+} + H^+ + Cit^{3-} \leftrightarrows HCaCit \quad \log K_6 = 9.3 \tag{11}$$

$$Ca^{2+} + 2H^+ + Cit^{3-} \leftrightarrows H_2CaCit^+ \quad \log K_7 = 9.3 \tag{12}$$

$$Mg^{2+} + Cit^{3-} \leftrightarrows MgCit^- \quad \log K_8 = 4.89 \tag{13}$$

$$Mg^{2+} + H^+ + Cit^{3-} \leftrightarrows HMgCit \quad \log K_9 = 8.9 \tag{14}$$

$$Mg^{2+} + 2H^+ + Cit^{3-} \leftrightarrows H_2MgCit^+ \quad \log K_{10} = 12.3 \tag{15}$$

Both anions Cit^{3-} and CO_3^{2-} are forming Ca(II)-precipitates according to reactions (16) and (17), respectively:

$$Ca_3Cit_2(s) \leftrightarrows 3\,Ca^{2+} + 2\,Cit^{3-} \quad \log K_{soc} = -17.8 \tag{16}$$

$$CaCO_3(s) \leftrightarrows Ca^{2+} + CO_3^{2-}\ \log K_{so} = -8.4 \quad (17)$$

The review of the geochemical databases does not report the formation of $Mg_3Cit_2(s)$ but it could be expected the formation of $MgCO_3(s)$. However it has been widely reported in the literature that the formation of $MgCO_3(s)$ ($pK_{s0} = 8.2$) in brines with high Ca(II) content is inhibited, although it is a more stable phase than $CaCO_3(s)$ minerals as calcite, aragonite or vaterite. For Ca-Citrate the formation mechanism is quite complicated due to complex ions and weak acid forms of citric acid in the solution (Vavrusova et al., 2017). However, above pH 7, complete citric acid dissociation occurs which reacts with Ca according to equilibrium (16).

To take into account the solution chemistry, both precipitation reactions were theoretically studied as function of pH to determine the more suitable conditions to evaluate the precipitation of both Ca(II) salts: $Ca_3Cit_2(s)$ and $CaCO_3(s)$. A speciation analysis was performed with the modelling software Hydra/Medusa (I. Puigdomenech, Chemical equilibrium software, Hydra/Medusa (2001)) and PHREEQC (USGS, 2017) codes and the results are described in Fig. 1.

As it is shown, the precipitation of $Ca_3Cit_2(s)$ is favoured at natural pH values of the brines, contrary the precipitation of $CaCO_3(s)$ occurs at pH values above, while the solubility of the precipitates decreases with increasing the solution pH. In both cases the acid-base properties of the precipitating anion could be used to control the crystal growth and, in the case of formation of calcium carbonate, it will be controlled by the ratio HCO_3^-/CO_3^{2-} by adjusting the pH of the solution. For $CaCO_3(s)$ it should be mentioned (although modelling data are not shown) that at pH values higher than 9.3 Mg(II) starts precipitating as brucite.

2.2. Dependence of precipitation reactions on temperature

The dependence of precipitate solubility from temperature is linked to the dependence of the equilibrium constant from temperature through the van't Hoff equation where the reaction enthalpy is related to the equilibrium (solid solute) ⇆ (solute in the saturated solution) which is influenced by the solute-solute interaction in the concentrate solution. In the case of low soluble salts, the limit solution enthalpy (which is the enthalpy variation to form a very diluted solution, where the solute-solute interactions are negligible) can be used in the van't Hoff equation. For $CaCO_3(s)$ and $MgCO_3(s)$ the limit ΔH_{sol} are −13.1 and −25.3 kJ/mol (at 25 °C), respectively. These values are the difference between the lattice enthalpy and the hydration enthalpy to form a very dilute solution. A negative value means a predominance of the hydration enthalpy, and, in particular, they show that magnesium ion is more hydrated than calcium. For other species that can be formed in the system the ΔH_{sol} are: $Mg(OH)_2(s)$, +2.3 kJ/mol; $Mg(SO_4).7H_2O(s)$ −90.9 kJ/mol; $CaSO_4(s)$ −19.2 kJ/mol. Considering that a negative ΔH_{sol} means exothermic reaction, from the Le Chatelier principle comes a solubility decrease with temperature increase. However, it must be considered that in low concentrated solutions, such as the brine, the solute-solute interactions can be also important so the limit ΔH_{sol} values can be only a guide but experiments on the temperature effects must be done.

2.3. Dependence of solubility from ionic strength: ion-ion interaction effects

The ionic strength (I) of the solution ($I = \frac{1}{2}\sum_{i=1}^{n} c_i z_i^2$, where c_i and z_i are the molar concentration and the ion charge of single ions, respectively), influences the solubility. Indeed, increasing the ion concentration the solute-solute interactions increase generating a discontinuity in the electric field so that the attraction among the precipitating ions is obstacled by the other ions and, as a result, the solubility increases.

The ion-ion interactions can be characterized by calculating the effective ion surface density (by Slater rule) [Silvestroni, 2020], ion hydration and Eigen association process (Akilan et al., 2006) of the precipitate formation in the complex multicomponent brine. The effective ion surface density (EISD = $EC/4\pi r^2$) is the ratio between the effective charge (EC) of an ion and the surface of the hydrated ion ($4\pi r^2$). For Mg^{2+} $EC_{Mg2+} = 12 - (0.85 \times 8 + 2) = +3.2$ and for Ca^{2+} $EC_{Ca2+} = 20 - (0.85 \times 8 + 10) = +3.2$, by applying the Slater rule, while the hydrated surfaces (HS) can be calculated knowing for Mg^{2+} the hydrated radius (4.76 Å) obtaining $HS_{Mg} = 284.6$ Å^2, and for Ca the hydrated radius of 2.95 Å and $HS_{Ca} = 109.3$ Å^2. So $EISD_{Mg} = 0.0112$ Å^{-2} and $EISD_{Ca} = 0.0293$ Å^{-2} which shows that the Ca hydrated ion has a EISD 2.6 times higher than Mg that means higher ability to attract negative ions. The EISD generally increases with temperature increase. For Ca ion the hydration number (HN), which is the average number of water molecules that bound sufficiently strong to the ion and become part of the solute, show a gradual decrease from 12 to 5 in the range of freezing point to 200 °C, respectively (Zavitsas, 2005). This means that it does not change too much in the interval 50 ± 20 °C used in the present work (HN values of 10.25 ± 0.70 assuming a linear decrease).

The precipitate formation is a process that can be understood considering the Eigen association process (Akilan et al., 2006). It foresees that free hydrated ions initially combine to form a double solvent-separated ion pair (2SIP) with their hydration sheaths thought to be essentially intact. This is followed by a sequential loss of water molecules from the coordination shells of the ions to form successively a solvent-shared ionic pair (SSIP) and ultimately a contact ion pair (CIP). This mechanism is thought to be a general description of the association

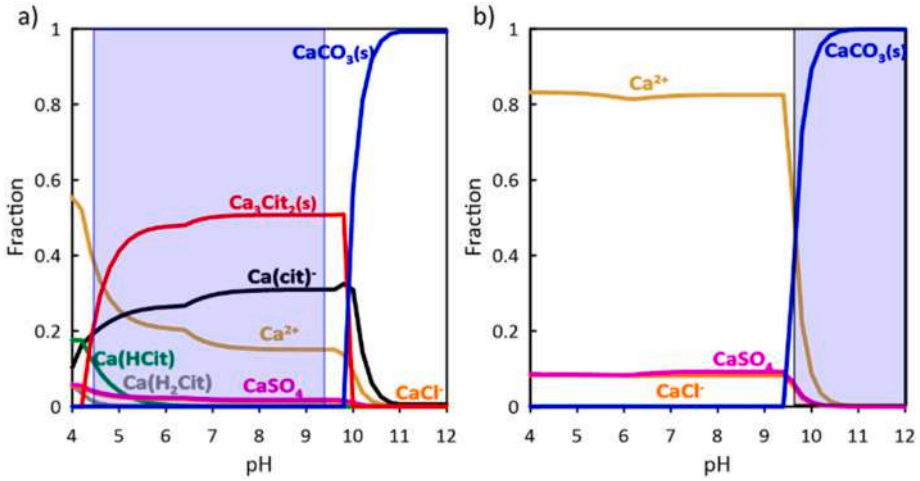

Fig. 1. Theoretical behaviour of Ca(II) precipitation with pH using the anions citrate (graph a) and carbonate (graph b). (a) Molar fraction for Ca(II) using an excess of citrate/Ca(II) = 5, (b) molar fraction for Ca(II) using an excess of carbonate/Ca(II) = 2. The brine solution used for simulation was the typical composition of a SWRO brine. Boxes included in both figures define the range where precipitation of $Ca_3Cit_2(s)$ and $CaCO_3(s)$ is thermodynamically favoured. Equilibrium diagrams were built by using Medusa Equilibrium Code and equilibrium constants are at 298K.

process for all strongly solvated ions in solution that generates a strong ionic bond forming clusters of aggregate particles or a lattice crystal. The number of water molecules in a crystal is generally higher at lower crystallization temperature.

2.4. Dependence of Ca(II) and Mg(II) precipitation on the molar ratio of the precipitating reagents

The reagents molar ratio influences the amount of precipitated Ca through the equilibriums (6) and (7) shifting them from right to left. In the case of $CaCO_3$ precipitation (which will be treated more extensively following), the minimum molar ratio is the reaction stoichiometry which is 1, but a little higher ratio CO_3^{2-}/Ca^{2+} is foreseen depending also on the intensity of ion-ion interactions. In particular, being the moles of Mg^{2+} in the synthetic brine, about 5 time more than Ca^{2+}, an inhibition of $CaCO_3$ precipitation is expected depending on the competition between the two ions for the CO_3^{2-} ion. This competition is also a function of the oversaturation ratio $OSR = Q_s/K_{s0}$ where Q_s is the solubility quotient, which is related to the concentration of the precipitating reagent added into the brine, and K_{s0} is the solubility constant.

3. Materials and methods

3.1. Reagents

Various salts were used to prepare synthetic solutions by dissolving them into Milli-Q water: $CaCl_2{\cdot}2H_2O$ (RCS grade, from Riedel de Haen), $MgCl_2{\cdot}6H_2O$ (>99%, from Panreac), Na_2SO_4 (ACS grade, from Sigma Aldrich), NaCl (>99%, from Sigma Aldrich), KCl (ACS grade, from Sigma Aldrich), $NaHCO_3$ (>99%, from Panreac), Na_2CO_3 (>99.5%, from Sigma Aldrich), Na_3Citr (anhydrous 99%, from Alfa Aesar).

Precipitation tests were designed having as a reference the synthetic brine composition reported in Table 1 where only salts of major ions were considered (SBp).

3.2. Ca(II) stock solutions for citrate precipitation tests

0.0215 M (Ca concentration in the brine) and 0.086 M (4 times of Ca concentration in brine) calcium stock solutions were prepared by dissolving $CaCl_2{\cdot}2H_2O$ in Milli-Q water.

1.35 M Na_3Citr solution was prepared as the precipitating agent by dissolving Na_3Citr in Milli-Q water.

Before mixing, the pH of both solutions was adjusted to 7.5 by adding 0.01M HCl or 0.01 M NaOH. The precipitation experiments were done in a batch reactor configuration (test tubes) with total volume of the mixed solutions 5 mL, the pH was adjusted as above described and stirring was done by a magnetic bar.

3.3. Ca(II) stock solutions for carbonate precipitation tests

Five different Ca stock solutions were prepared according to ionic compositions reported in Table 2 where in the "Ca+Na(0.33M)" solution the Mg(II) content of "Ca+Mg" solution was mimicked with NaCl by calculating its ionic strength while in the "Ca+Na(1.37M)" solution the major ions content of brine, except Ca, was mimicked with NaCl by calculating the ionic strength.

Table 1
Concentration of synthetic brine (major ions).

Reagent	g/L	mol/L
Na_2SO_4	8.38	0.0590
$NaHCO_3$	0.13	0.00155
NaCl	48.15	0.824
KCl	1.53	0.0205
$MgCl_2$	10.98	0.115
$CaCl_2$	2.38	0.0215
Na_2CO_3	0.042	0.0004

Table 2
Concentration of Ca stock solutions for carbonate precipitation tests.

Code	Ca(g/L)	Ca (mol/L)	Mg (g/L)	Mg (mol/L)	Na (g/L)	Na (mol/L)
Ca_Only	0.86	0.0215	–	–	–	–
Ca+Mg (0.11M)	0.86	0.0215	2.79	0.115	–	–
Ca+Na (0.33M)	0.86	0.0215	–	–	7.59	0.33
Ca+Na (1.37M)	0.86	0.0215	–	–	31.51	1.37
SBp			See Table 1			

Three stock solutions containing the precipitating agent $NaHCO_3$ (1.07 M) were prepared at three different pH (8.5, 9.0, and 9.5) by dissolving $NaHCO_3$ in Milli-Q water. 2.36 M Na_2CO_3 stock solution was prepared by dissolving Na_2CO_3 in Milli-Q water. The pH of the solutions was adjusted by addition of diluted NaOH or HCl.

The Ca(II) stock solutions were mixed with $NaHCO_3$ or Na_2CO_3 stock solutions in appropriate portions to conduct designed $CaCO_3$ precipitation experiments. The precipitation experiments were done in a batch reactor configuration (test tubes) with total volume of the mixed solutions 5 mL, the pH was adjusted as above described and stirring was done by a magnetic bar.

3.4. Analytical methods

The pH values were measured with a pH meter (WTW Inolab Terminal Level 3, Germany). Quantification of Ca^{2+} and Mg^{2+} in the supernatant solutions was made by High-Resolution Continuum Source Atomic Absorption Spectrometer (HR-CS AAS) ContrAA 700 (Analytik Jena AG, Germany) with a high-intensity Xe short-arc lamp as continuum source, calibrated with ICP multi-element IV standard solution from Merck. Method parameters (i.e. fuel flow and burner height), obtained by the flame automatic optimization procedure for the determination of Ca and Mg, were applied. The absorbance measurements were performed using the spectral lines 422.67 nm and 202.58 nm for Ca and Mg determination, respectively. Supernatant samples (volume of 25–50 μL) were withdrawn and properly diluted with Milli-Q water to the calibration range of atomic absorption, i.e. 0-3.5 mg/L, and acidified with 1% v/v HCl. In case of the tests performed with agitation, to avoid the possible withdrawal of suspended precipitate in the supernatant, stirring was stopped 10 min before sampling.

Analytical determination concerned mainly calcium and magnesium ions being them involved in the precipitation process, while the effect of the other ions was tested by analyzing with EDX the precipitate samples.

3.4.1. X-ray diffraction on solid samples precipitates

At this stage of the project particle size of the precipitates was not measured. Precipitates were analyzed by powder X-ray diffraction (XRD) to determine the composition and the major mineral phases of the crystalline content in the samples. The samples were homogenized and, if necessary, ground, before analysis. Analyses were made on a Bruker® D5005 X-Ray Diffractometer in θ–θ mode with Cu Kα radiation. Repeated continuous scans were performed on rotating samples in the 2θ range 0–60° at a rate of 0.025°/18 s. Granular precipitates were also observed under a JEOL® JSM840 Field Emission Scanning Electron Microscope with Oxford Link® Energy Dispersive System (SEM-EDS).

4. Results and discussion

The brine produced by a RO seawater plant is a source of numerous compounds and its further treatment permits to reach the objective of near zero liquid discharge (NZLD) by recovering water and dissolved salts. One of the first step to design a brine valorization process is the

selective Ca and Mg removal/recovery to avoid scaling problems in the successive treatments and to recover valuable minerals. Conventional softening methods, based on direct addition of quicklime (CaO), lime ($Ca(OH)_2$), sodium hydroxide (NaOH), soda ash (Na_2CO_3) between others, lead to Mg^{2+} loss by incorporation into calcite. However, it must be considered that the $CaCO_3$(s) mineral phase precipitate could be calcite, aragonite or vaterite or dolomite ($CaMg(CO_3)_2$(s)) depending on the precipitation conditions. According to the Mg/Ca molar ratio (5/1) of the synthetic brine used in this work, it could be expected the precipitation as aragonite where Mg(II) is not incorporated (Morse et al., 1997) into the crystal structure due to sizes limitations. Indeed, in par. 2.2 is reported that Mg^{2+} hydrated radius is 4.76 Å while the Ca^{2+} hydrated radius is 2.95 Å. Some authors used precipitation as carbonates to remove Ca^{2+} from Mg^{2+} obtaining Ca removal of 94%–96% with a Mg loss >60% at 60 °C (Casas et al., 2014) and Ca removal <85.4% with a Mg loss <6.7% (Wang et al., 2020) at 85 °C. Following the results on three tested precipitation reagents (Na citrate ($Na_3C_6H_5O_7$), Na_2CO_3 and $NaHCO_3$) are presented and discussed.

4.1. Ca(II) precipitation by citrate solutions

Sodium citrate was tested to precipitate Ca(II) as calcium citrate, which is a possible valuable product from calcium removal. Solutions containing only $CaCl_2$ at a concentration of the brine (0.86 g Ca/L) and at a concentration 4 times the brine, were tested at 30 and 60 °C using a molar ratio Cit/Ca = 2 and analysing the Ca(II) content in the supernatant in the time. The corresponding OSR values were 1.2×10^{10} and 1.2×10^{13} for the lowest (21.5 mM) and the highest (86 mM) calcium concentrations, respectively, reported in Fig. 2. From this figure it can be seen that Ca(II) removal from a solution at low concentration (such that of the brine) follows a very slow kinetics even at high temperature (60 °C). Indeed, the higher is the initial Ca^{2+} concentration (e. g. 4 times the brine) the higher is Q_s for a same precipitant concentration meaning, as opposite, the requirement of a lower precipitant concentration to obtain the same precipitation efficiency. This behaviour is particularly important when the citrate ion is used as precipitating reagent because, at high concentration, it reacts with the precipitate forming soluble complex ($CaCit^-$) species increasing its solubility (Vavrusova et al., 2017). However, the possibility to further concentrate the brine (e. g., evaporation, nanofiltration, etc.) has not been considered in this work because the focus was only the brine as such.

The measured Ca(II) removal values at 30 °C in Fig. 2, once equilibrium was attained (e.g. 30 h for experiments at 21.5 mM (0.88 g Ca/L) and extrapolated at long time for the experiment at 86 mM (3.52 g Ca/L), were compared with the predicted values, using the Medusa Numerical Code, shown in Fig. 3.

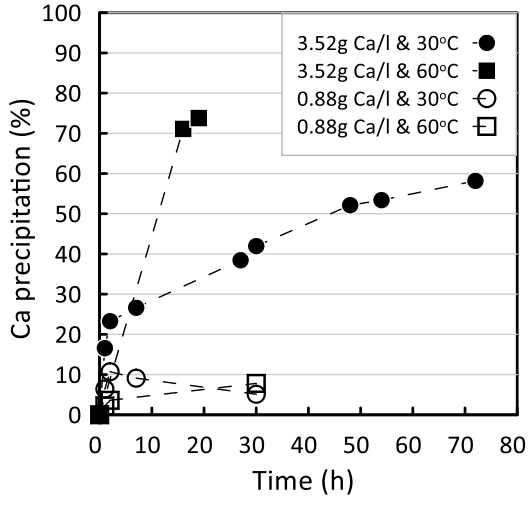

Fig. 2. Effect of Ca concentration and temperature on Ca_3Cit_2(s) precipitation (Solutions were 0.0215 M and 0.086 M Ca^{2+}, precipitation agent Na_3Cit, molar ratio Cit/Ca = 2, pH of two solutions adjusted to 7.5 by adding 0.01 M NaOH).

In Fig. 3 the experimental values on Ca(II) as Ca_3Cit_2(s) for 86 mM (3.52 gCa/L) of Ca^{2+} are well predicted (extrapolating the related curve in Fig. 2 at long time to reach equilibrium) while for 21.5 mM (0.88 gCa/L) measured values were lower than those predicted by Medusa.

Because of low efficiency and slow precipitation kinetics, other types of precipitants were considered as an alternative to sodium citrate; such as carbonate, oxalate and phosphate. The solubility of the respective Ca and Mg salts was studied using the solubility values reported in Table 3. To foresee the possibility to remove maximum Ca with minimum Mg removal, the ratio of the solubility between the respective Mg and Ca salt was considered. As it can be observed, the solubility ratio of Mg/Ca salts of carbonate is significantly higher, thus soluble carbonate salts such as sodium carbonate and sodium bicarbonate were considered as possible precipitating agents.

4.2. Ca(II) precipitation as carbonate using sodium carbonate

Some tests using the Ca+Mg(0.11M) solution (see Table 2), to which a 2.36 M solution of sodium carbonate was added, were carried out and the results are reported in Fig. 4. It can be observed that the Ca precipitation percentage increases with increasing the molar ratio CO_3/Ca till about 98% but Mg precipitation is practically independent from the molar ratio (about 25% for all the ratios). This can be ascribed to the high initial pH of the sodium carbonate solution (pH = 12) that induces $Mg(OH)_2$ precipitation as already described (Casas et al., 2014), despite the final pH of the solutions were in the range 9.75 ± 0.15.

Results on Ca(II) removal with Na_2CO_3 solutions from Fig. 4 were compared with the predictions provided by PHREEQC as shown in Fig. 5 by simulating mixing of solutions volumes.

In Fig. 5b) it can be observed that Ca(II) removal ratios as $CaCO_3$(s) is reproducing very accurately the removal rates described in Fig. 4, and then, for process design purposes, the use of PhreeqC program could be a simple solution to describe the removal of Ca(II). Instead, removal ratios of Mg(II) were not well predicted (about zero in Fig. 5a) versus about 25% in Fig. 4). This last value can be explained by the formation of Mg $(OH)_2$(s) just at the beginning of the precipitant addition (pH 12) while in the model the reagent mixing foresee already the equilibrium pH. The %Mg precipitation in Fig. 4 cannot be justified by the $MgCO_3$(s) formation because the substitution of Ca(II) by Mg(II) in the precipitated $CaCO_3$(s), to form the mineral phase calcite, cannot be foreseen because in the experimental conditions the aragonite is formed as reported by Morse et al. (1997). Additionally, analysis of the samples by FSEM-EDAX and by XRD did not detect any mineral phase of Mg and carbonate. Only $CaCO_3$(s) in the form of aragonite was detected.

4.3. Ca(II) precipitation as carbonate using sodium hydrogen carbonate

In the equilibrium HCO_3^-/CO_3^{2-} reported in eq. (5) the hydrogen carbonate ion can be considered a reservoir of carbonate ion by shifting the equilibrium when the carbonate reacts with Ca(II) according to equilibrium (17). The ratio $[CO_3^{2-}]/[HCO_3^-]$ is in the range 0.056–0.56 for a pH range of 9–10, respectively according to the equilibrium constant K_{a2}. Despite this ratio is low, the shift of the equilibrium promotes a gradual calcium carbonate precipitation without a local excess of carbonate favouring the formation of aragonite and consequently reducing the substitution of Ca (II) by Mg(II) as occurs when calcite is formed and, furthermore, the pH below 10 reduces $Mg(OH)_2$ precipitation increasing the selectivity factors compared to sodium carbonate addition.

4.3.1. Effect of ionic strength (IS) and Mg(II) competition in Ca(II) precipitation

Because $CaCO_3$ solubility (or, its precipitation) can be dependent on the Mg^{2+} presence and other ion-ion interactions through the ionic

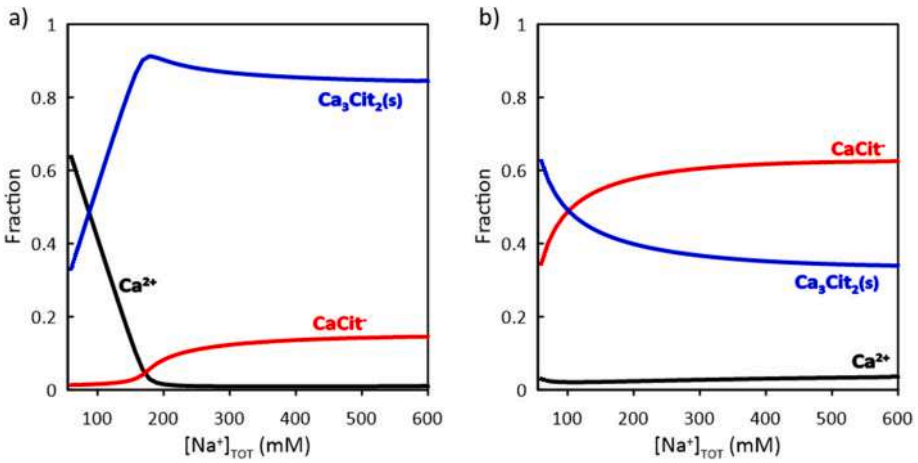

Fig. 3. Molar fraction diagrams for Ca^{2+} as function of total sodium citrate in the evaluated range at pH = 7.5 for (a) 21.5 mM and (b) 86 mM Ca^{2+} concentration referring to conditions described in Fig. 2. Equilibrium diagrams were built by using Medusa Equilibrium Code and equilibrium constants are at 298K.

Table 3
Solubility of Ca and Mg carbonate, oxalate and phosphate salts and their solubility ratio.

Precipitant	Calcium precipitate Formula	Solubility (g/100 g H_2O)	Magnesium precipitate Formula	Solubility (g/100 g H_2O)	Solubility ratio Mg salt/Ca salt
Carbonate	$CaCO_3(s)$	0.00066	$MgCO_3(s)$	0.18	272
Oxalate	$CaC_2O_4(s)$	0.00061	$MgC_2O_4(s)$	0.038	62
Phosphate	$Ca_3(PO_4)_2(s)$	0.00012	$Mg_3(PO_4)_2{\cdot}5H_2O(s)$	0.00009	0.75

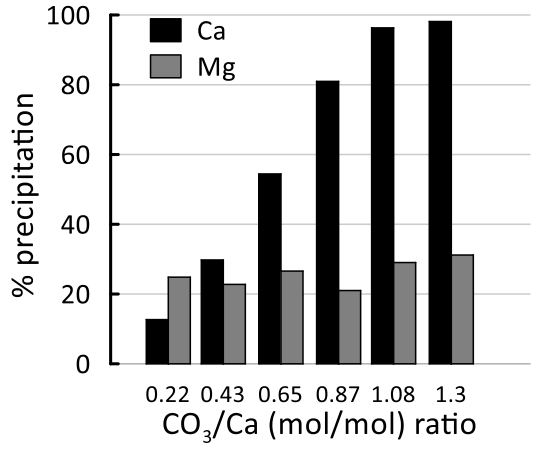

Fig. 4. Precipitation percentage of Ca and Mg by increasing the CO_3/Ca molar ratio (Solutions: 0.0215M $CaCl_2$, 0.115 M $MgCl_2$, 2.36 M Na_2CO_3; room temperature (24 °C), pH_{eq} 9.75 ± 0.15).

strength (IS) of the solution, some tests with and without Mg^{2+} presence and at various IS values were carried out at 25 and 60 °C. From Fig. 6 it can be seen that Mg^{2+} presence in solution (0.115 M which is the Mg(II) concentration of SB) decreases the Ca precipitation because of competition between Ca and Mg as theoretically described previously in section 2.

In particular, Fig. 6 confirms (at both temperatures) that the lower Ca precipitation ratio was caused by Mg competition and not by its ionic strength (0.33M). Indeed, the precipitation trend for both the Ca+Na (0.33M) solutions, where $MgCl_2$ has been substituted by NaCl with the same IS, is very close to the Ca precipitation curve. However, an effect of the IS can be seen only after 3 h showing a lower Ca precipitation ratio. In addition, the Ca(II) precipitation curve for Ca+Na(1.37M) solutions, where NaCl at the same total IS of the SBp has been added to the Ca(II) solution, is practically overlapped with the precipitation curve for Ca+Na(0.33M) solutions resulting an insignificant effect on Ca precipitation in the IS range 0.33–1.37 M. Therefore, the assumption of considering the SBp as a low concentrated solution (see paragraph 2.) is also confirmed by this negligible effect.

4.3.2. Effect of pH on Ca(II) and Mg(II) precipitation in the SB solution

When $NaHCO_3$ is used as precipitating reagent, the important role of pH on the $[CO_3^{2-}]/[HCO_3^-]$ ratio must be considered. As reported before, the pH should be between 9 and 10 to obtain a significant CO_3^{2-} concentration, and, to avoid/reduce $Mg(OH)_2$ precipitation. For this reason, the experiments were carried out at pH 9 and 9.5. In Fig. 7 it can be seen that at 60 °C the difference of Ca precipitation between the two pH is more significant than the experiments carried out at room temperature.

This behaviour can be ascribed to the higher reactivity between calcium and carbonate ions (e.g. higher solubility constant log K_{s0} (60 °C)) at elevated temperature and easier loss of water molecules from the coordination shells of the ions to form a contact ion pair by the Eigen mechanism).

Results on Ca(II) precipitation ratio from Fig. 7 (as dots) were compared with the predictions (solid lines) provided by PhreeqC shown in Fig. 8. Predicted values were obtained by mixing the two solutions used in the precipitation assays as it is described in the experimental section (e.g. mixing 5 mL of SBp with 0.21 mL of $NaHCO_3$ at different initial pHs).

PhreeqC predictions were done using Pitzer and llnl data bases and assuming that only aragonite precipitated as it was confirmed by DRX. It was observed that Ca(II) precipitation ratios provided by llnl data base (results presented in Fig. 8) gave a much better description than the values predicted by the Pitzer data base (data not shown). Differences in the predicted values are associated to the fact that Pitzer data does not consider the aqueous species between Ca(II)/Mg(II) with CO_3^{2-} ions (e.g. $NaHCO_{3(aq)}$, $MgHCO_3^+$, $CaHCO_3^+$, $MgCO_{3(aq)}$, $CaCO_{3(aq)}$ and $NaCO_3^-$). The higher Ca(II) precipitation predicted values, in comparison with the measured values, are explained by the fact that predictions assume that equilibrium was reached while, in the experiments, values at 6 h are not still equilibrium.

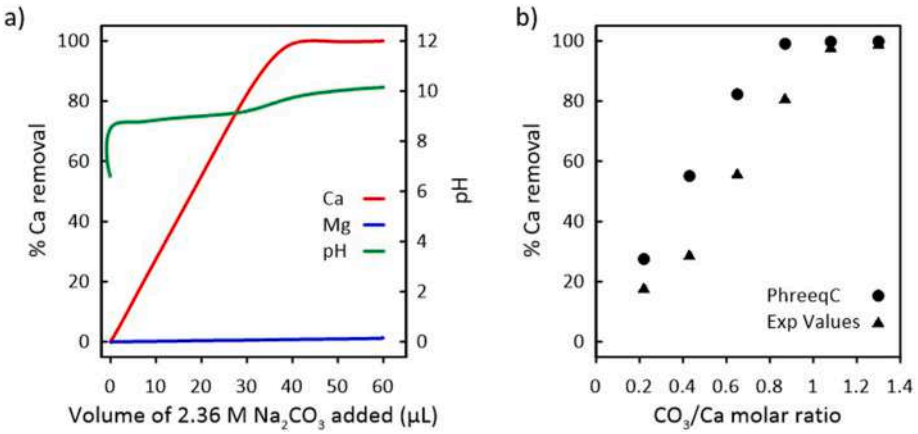

Fig. 5. (a) Precipitation percentage of Ca(II) and Mg(II) and equilibrium pH, as a function of total sodium carbonate, built by using PhreeqC modelling program in the evaluated range in experiments shown in Fig. 4; (b) comparison of molar fractions for Ca(II) between model (blue) and experimental values (red). (For interpretation of the references to colour in this figure legend, the reader is referred to the Web version of this article.)

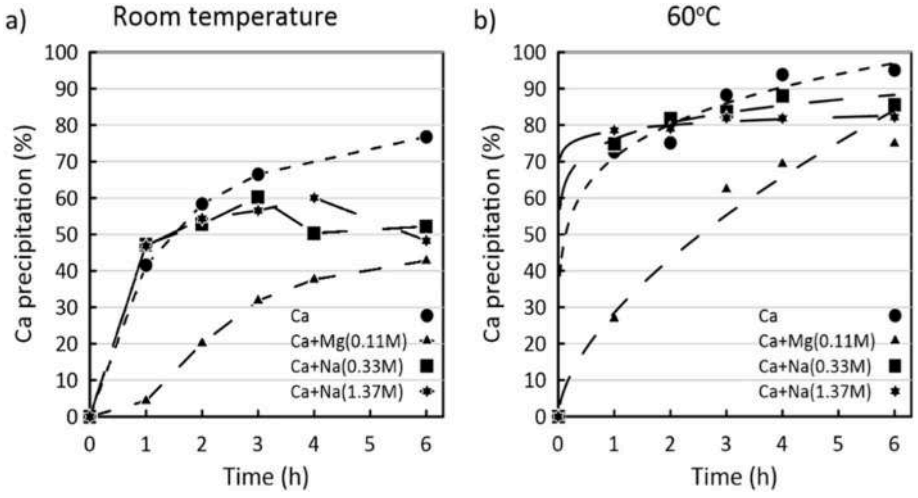

Fig. 6. Effect of Mg and ionic strength (IS) on Ca(II) precipitation at (a) room temperature (20 °C) and (b) 60 °C ($pH_{NaHCO3} = 9.0$ and $HCO_3^-/Ca^{2+} = 2$; Ca: 0.0215 M $CaCl_2$; Ca+Mg(0.11M): 0.0215 M $CaCl_2$ + 0.115 M $MgCl_2$; Ca+Na(0.33M): 0.0215 M $CaCl_2$ + 0.33 M NaCl and Ca+Na (1.37M): 0.0215M $CaCl_2$ + 1.37 M NaCl).

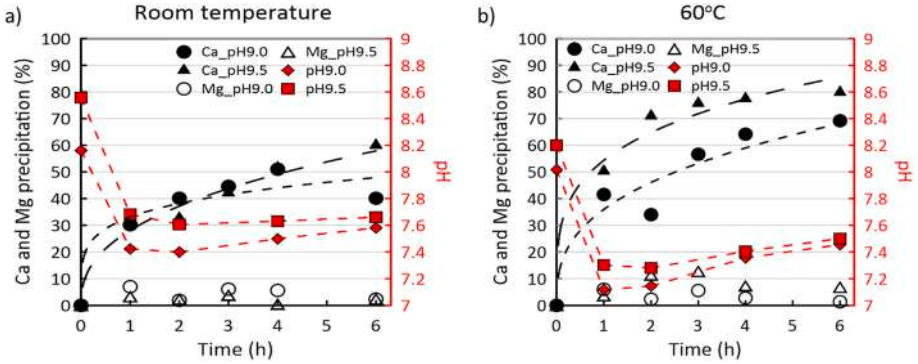

Fig. 7. Effect of pH and pH variation during Ca and Mg precipitation in SBp solution at a) (left) room temperature (20 °C) and b) (right) 60 °C at $HCO_3^-/Ca^{2+} = 2$.

4.3.3. Effect of the molar ratio $[CO_3^{2-}]/[Ca^{2+}]$ on Ca(II) and Mg(II) precipitation in the SB solution

The molar ratio ($R = [CO_3^{2-}]/[Ca^{2+}]$ of the Ca-CO_3 equilibrium reaction (17) is 1:1. It is well known that increasing the equilibrium concentration of a reagent the reaction shifts to the products according to Le Chatelier principle, so, in Fig. 9, the Ca precipitation increases by increasing R. At 6 h the average solubility quotient Q_s for all the four R values is $(1.66 \pm 0.23) \times 10^{-4}$ that gives an OSR 17000–20000.

Despite this value is still high (but it was higher at time zero), the trend of precipitation reaction curves is approaching a plateau (Fig. 9). So, it can be considered as a characteristic parameter that includes both the negative effects of Mg competition and ionic strength on Ca precipitation meaning that a significant Ca precipitation is not expected below this value.

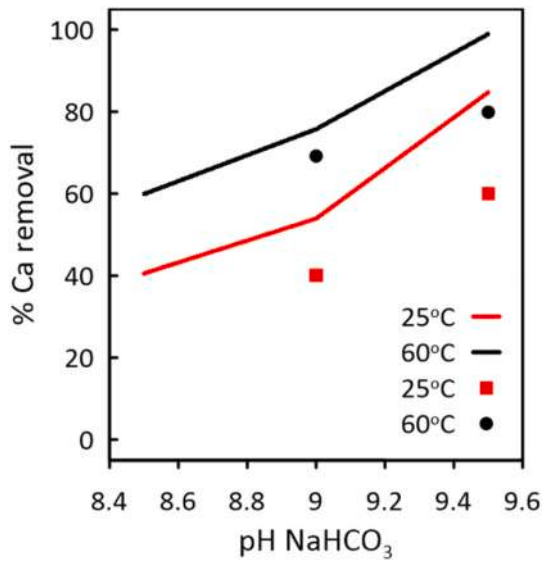

Fig. 8. Comparison of Ca(II) precipitation ratio, as a function of the initial pH, predicted by PHREEQC at 25 °C and 60 °C (solid lines) using the llnl data base and the values (square and lozenge points) of experimental data shown in Fig. 7. Values of volumes and the initial concentrations of the solutions are described in the experimental section.

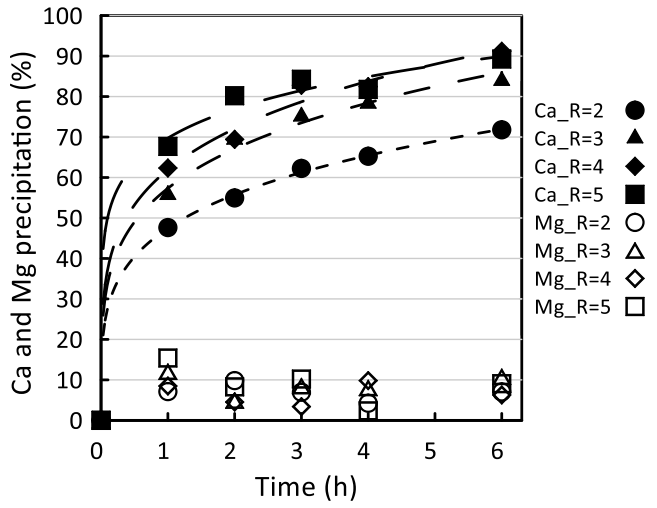

Fig. 9. Effect of molar ratio R on Ca and Mg precipitation in the SBp solution (pH_{NaHCO3} = 9.0, T = 60 °C).

Fig. 9 is also related to the settling curves for Ca and Mg precipitation (expressed as precipitation percentage) showing a general increase of Ca precipitation and a general decrease of Mg precipitation during the aging process in the time. The magnesium behaviour can be interpreted as initial $MgCO_{3(S)}$ nanocrystals co-precipitation that were partially dissolved in the time because of the CO_3^{2-} concentration decrease (reacting it with Ca^{2+}).

4.3.4. Effect of temperature on Ca(II) and Mg(II) precipitation in the SBp solution

According to the Eigen mechanism of precipitate formation, a higher kinetics of the $CaCO_3$ formation can be expected by increasing temperature because of the easier loss of water molecules from the coordination shells of the ions to form a contact ion pair (ionic bond between Ca^{2+} and CO_3^{2-}). Because a faster kinetics has been observed at 60 °C compared to the room temperature, further experiments were conducted in the range 50–70 °C (Fig. 10).

An increase of 0.5–1% Ca precipitation/°C has been calculated from these data. So, assuming the same trend is applicable at different temperatures, it can be foreseen, for example, 95 %Ca precipitation in 2 h at 95 °C. The increase of %Ca precipitation with increasing temperature is justified by the decrease of the constant of the equilibrium (17) with the temperature because of the negative reaction enthalpy (limit ΔH_{sol} of $CaCO_3(s)$ = −13.1 kJ/mol, at 25 °C). This positive effect of temperature agrees with that one obtained by Choi et al. (2018) in the case of Ca(II) precipitation as $CaSO_4(s)$. In such case also, the authors attributed this trend to the change in solubility by increasing the temperature.

4.3.5. Effect of agitation on Ca(II) precipitation in the SBp solution

The agitation effect on reaction kinetics at 60 and 70 °C has been studied at the molar ratios R = 3 and 4 and the results are summarized in Fig. 11. While the agitation effect is not important at longer time (6 h in this work), showing a %Ca precipitation practically around 90% in all cases, it is an important parameter at short reaction times.

Indeed, in Fig. 11, it can be seen about 90 %Ca precipitation in 1 h with a suitable mixing of the suspension. This positive effect of agitation on the formation of the crystals and then on %Ca precipitation agrees with the results of Choi et al. (2018) on $CaSO_4$ crystal formation and precipitation. On the basis of their studies they concluded that agitation positively affects the formation and growth of crystals, evidencing that it is controlled by agitation speed. However, it should be considered that nucleation and growth in precipitation systems should be studied by considering how micromixing affects those processes occurring at molecular scale (Elduayen-Echave et al., 2021). On the other side, it must be considered that in absence of external mechanical stirring, the diffusion of the ions in the solution is the main mechanism that tends to standardize the concentrations. However, the diffusion rate is significantly slower than the agitation. The diffusion coefficient (D) could be calculated by eq (18):

$$D = RT/\ N \times f = kT/f \quad (18)$$

where R is the gas constant, N the Avogadro number, k the Boltzmann constant, f the friction coefficient and T the absolute temperature. If the species that diffuses is a sphere, the friction coefficient could be calculated from the Stokes law as described by equation (19):

$$f = 6\pi\eta r \quad (19)$$

where η is the medium viscosity and r the radius of the species that diffuses (it is the aqueous ionic radii which is calculated from published

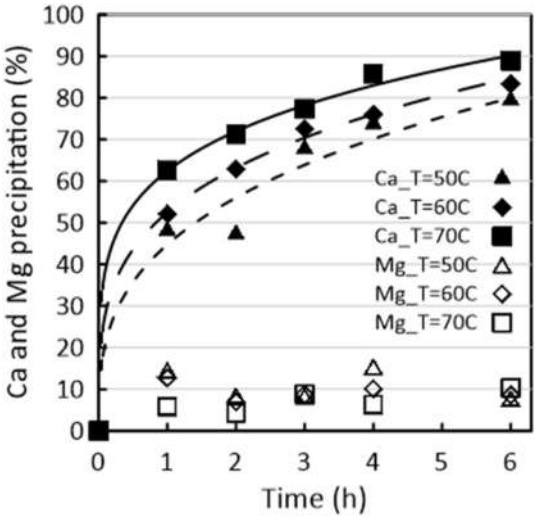

Fig. 10. Effect of temperature on Ca and Mg precipitation in the SBp solution (pH_{NaHCO3} = 9.0 and R = 3).

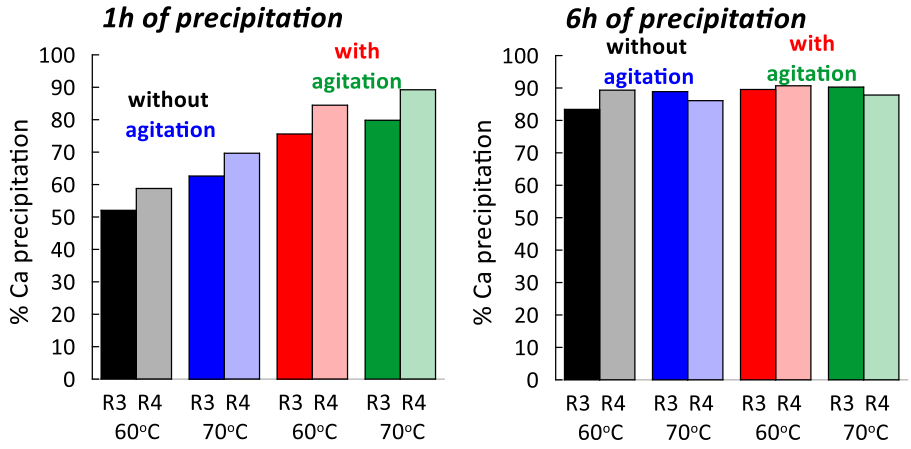

Fig. 11. Effect of agitation on Ca precipitation in the SBp solution (pH_{NaHCO3} = 9.0).

data of the average distances between the ions and the nearest water molecules, obtained by diffraction and computer simulation methods). Thus, the diffusion coefficient is proportional to temperature and inversely proportional to η and to the ion size r. This means that increase of temperature acts at molecular level promoting ion diffusion. This effect can be alone or in addition to the mechanical stirring, if it is also present.

4.3.6. *Comparison of Ca(II) removal performance with literature data*

The approach of selective Ca(II) precipitation, studied in the present work, on our knowledge, has been studied only by Wang et al. (2020). They obtained comparable results working at a temperature (85 °C) higher than the ones we investigated (from room temperature to 70 °C). In Table 4 the main parameters are compared.

Despite the results of Ca and Mg precipitation in the two studies are quite similar, the approach used in the present study, consisting in the use of sodium hydrogen carbonate, permitted the pH control of the precipitation process and operated at a lower temperature. The temperature of the brine after calcium removal (60–70 °C) was of interest for planning as subsequent stage a membrane distillation operation as described in the next section.

4.4. *A possible treatment train for clean production of water and minerals from SWRO desalination brines*

A conceptual approach, able to use the results of the present work, is schematized in Fig. 12.

The brine discharged by the RO plant is heated to 60–70 °C (using solar collectors to make it more attractive from a sustainable point of view) and, after Ca removal by the precipitation at controlled pH, it is sent to a membrane distillation (MD) unit by taking advantage of the stream at high temperature. It is known that water flux of the membrane distillation process is significantly reduced by inorganic scaling mainly caused by calcium-based compounds which crystals are deposited on the membrane surface. Although the concentration of feed solution does not reach the super saturation, these crystals act as nuclei, resulting in the easy growth of crystals becoming an obstacle in improving the water recovery ratio. The calcium precipitation from reverse osmosis seawater desalination brines, before feeding to the membrane distillation process, studied in the present work, can overcome/reduce this scaling problem. Consequently, the brine valorization process can be improved by improving the operational and economic efficiency of membrane distillation. From the MD unit, water recovery and a concentrate mixture of the various elements, initially present in the seawater at very low concentration, are obtained. The very concentrated salts media can be further processed for recovering the components (as for example Mg (II) mineral which is the main component of this stream) together with NaCl.

Table 4
Comparison of parameters used by Wang et al. and this work.

Parameters	Wang et al. (2020)	This work	
	Carbonate	Carbonate	Bicarbonate
Temperature (°C)	85	RT*	70
Stirring rate (RPM)	200	–	yes
Reaction time (h)	0.67	1–6	1
Na_2CO_3/Ca^{2+}	1	1.2	–
HCO_3^-/Ca^{2+}	–	–	4
%Ca precipitation	85	98	91
%Mg precipitation	7	33	7

•* RT: Room temperature.

5. Conclusions

To design clean processes, a deep understanding of the fundamentals of the involved chemical processes is required. In the present work, the study of the chemical aspects of calcium removal from a synthetic brine (SBp), simulating the average brine obtained from reverse osmosis plants, has been strictly coupled between theory and experiments. The chemical basis of the precipitation processes and ion-ion interactions based on the effective ion surface density (e.g. Slater rule), ion hydration, Eigen association process of the precipitation reaction permitted a clear understanding of the experimental results. In particular, the calculation of the effective ion surface density (EISD) showed that the Ca^{2+} ion is 2.6 times more reactive than Mg^{2+} but, from the experiments, it has also been shown that competition between Mg^{2+} and Ca^{2+} ions with the carbonate ion hinder the Ca^{2+} precipitation as carbonate. For the three different precipitation reagents tested ($Na_3C_6H_5O_7$, Na_2CO_3 and $NaHCO_3$) it has been observed that: i) Ca precipitation as citrate is partial as even in excess of citrate anion the formation of a strong complex $CaCit^-$ hinders the precipitation of Ca in the SBp, ii) for sodium carbonate, because of the high initial pH, a significant $Mg(OH)_2$ precipitation is obtained, while iii) use of sodium hydrogen carbonate, because of the pH control below that of magnesium hydroxide precipitation, reduces Mg loss in the precipitated $CaCO_3$(s). The chemical speciation of Ca and Mg precipitation, by using geochemical numerical codes (e.g. Medusa, PHREEQC) showed good agreement of predicted values with the experimental results.

At pH 9.0, temperature of 60–70 °C, molar ratio HCO_3^-/Ca = 3, a Ca removal efficiency greater than 90% with a Mg loss below 7% were obtained. These results are of potential interest to design a NZLD process for brine valorisation treatment.

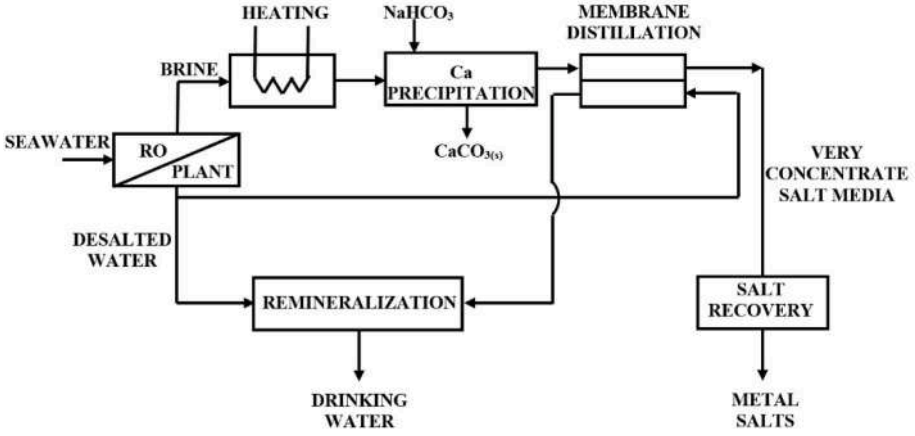

Fig. 12. Conceptual scheme of brine valorisation by previous Ca removal for approaching NZLD.

CRediT authorship contribution statement

Raffaele Molinari: Conceptualization, Methodology, Writing – original draft, Writing – review & editing, Supervision. **Ahmet Halil Avci:** Investigation, Methodology, Visualization, Writing – original draft. **Pietro Argurio:** Investigation, Visualization, Writing – original draft. **Efrem Curcio:** Writing – review & editing. **Sandra Meca:** Funding acquisition, Software. **Mireia Plà-Castellana:** Software, Validation. **Jose Luis Cortina:** Software, Validation, Writing – review & editing, Supervision.

Declaration of competing interest

The authors declare that they have no known competing financial interests or personal relationships that could have appeared to influence the work reported in this paper.

Acknowledgements

The financial support of European Union within H2020-SC5-2019-2 SEA4VALUE project (https://sea4value.eu/) under grant agreement ID 869703 is acknowledged. Authors thanks J. Lopez and C. Ayora for their help with PHREEQC data bases from sea water brines.

References

Akilan, C., Rohman, N., Hefter, G., Buchner, R., 2006. Temperature effects on ion association and hydratation in MgSO4 by dielectric spectroscopy. Chem. Phys. Chem. 7, 2319–2330. https://doi.org/10.1002/cphc.200600342.

Antony, A., Low, J.H., Gray, S., Childress, A.E., Le-Clech, P., Leslie, G., 2011. Scale formation and control in high pressure membrane water treatment systems: a review. J. Membrane Sci. 383, 1–16. https://doi.org/10.1016/j.memsci.2011.08.054.

Badruzzaman, M., Voutchkov, N., Weinrich, L., Jacangelo, J.G., 2019. Selection of pretreatment technologies for seawater reverse osmosis plants: a review. Desalination 449, 78–91. https://doi.org/10.1016/j.desal.2018.10.006.

Bang, J.-H., Yoo, Y., Lee, S.-W., Song, K., Chae, S., 2017. CO_2 Mineralization Using Brine Discharged from a Seawater Desalination Plant. Minerals 7, 207. https://doi.org/10.3390/min7110207.

Bouchrit, R., Boubakri, A., Hafiane, A., Bouguecha, S.A.-T., 2015. Direct contact membrane distillation: capability to treat hyper-saline solution. Desalination 376, 117–129. https://doi.org/10.1016/j.desal.2015.08.014.

Casas, S., Aladjem, C., Larrotcha, E., Gilbert, O., Valderrama, C., Cortina, J.L., 2014. Valorisation of Ca and Mg by-products from mining and seawater desalination brines for water treatment applications. J. Chem. Technol Biotechnol 89, 872–883. https://doi.org/10.1002/jctb.4326.

Chen, T., Neville, A., Yuan, M., 2006. Influence of Mg^{2+} on $CaCO_3$ formation-bulk precipitation and surface deposition. Chem. Eng. Sci. 61, 5318–5327. https://doi.org/10.1016/j.ces.2006.04.007.

Choi, Y., Naidu, G., Jeong, S., Lee, S., Vigneswaran, S., 2018. Effect of chemical and physical factors on the crystallization of calcium sulfate in seawater reverse osmosis brine. Desalination 426, 78–87. https://doi.org/10.1016/j.desal.2017.10.037.

Drioli, E., Curcio, E., Criscuoli, A., Di Profio, G., 2004. Integrated system for recovery of $CaCO_3$, NaCl and $MgSO_4{\cdot}7H_2O$ from nanofiltration retentate. J Membrane Sci 239, 27–38. https://doi.org/10.1016/j.memsci.2003.09.028.

Elduayen-Echave, B., Lizarralde, I., Schneider, P.A., Ayesa, E., Larraona, G.S., Grau, P., 2021. Inclusion of shear rate effects in the kinetics of a discretized population balance model: application to struvite precipitation. Water Res 200, 117242. https://doi.org/10.1016/j.watres.2021.117242.

European Commission, 2020. Study on the EU's List of Critical Raw Materials – Final Report. Publications Office of the European Union, Luxembourg, ISBN 978-92-76-21049-8. https://doi.org/10.2873/11619.

Giwa, A., Dufour, V., Al Marzooqi, F., Al Kaabi, M., Hasan, S.W., 2017. Brine management methods: recent innovations and current status. Desalination 407, 1–23. https://doi.org/10.1016/j.desal.2016.12.008.

International Desalination Association. https://idadesal.org/. (Accessed 30 June 2021).

Loganathan, P., Naidu, G., Vigneswaran, S., 2017. Mining valuable minerals from seawater: a critical review. Environ. Sci.: Water Res. Technol. 3, 37–53. https://doi.org/10.1039/C6EW00268D.

Martinetti, C.R., Childress, A.E., Cath, T.Y., 2009. High recovery of concentrated RO brines using forward osmosis and membrane distillation. J. Membr. Sci. 331, 31–39. https://doi.org/10.1016/j.memsci.2009.01.003.

Mero, J.L., 1965. The mineral resources of the sea. Geological Magazine 102 (6), 565. https://doi.org/10.1017/S0016756800000339.

Morse, J.W., Wang, Q., Tsio, M.Y., 1997. Influences of temperature and Mg:Ca ratio on $CaCO_3$ precipitation from seawater. Geology 25, 85–87. https://doi.org/10.1130/0091-7613(1997)025<0085:IOTAMC>2.3.CO;2.

Natasha, N.C., Lalasari, L.H., 2017. Calcium extraction from brine water and seawater using oxalic acid. AIP Conference Proceedings 1805, 070002. https://doi.org/10.1063/1.4974443.

Quist-Jensen, C.A., Ali, A., Mondal, S., Macedonio, F., Drioli, E., 2016. A study of membrane distillation and crystallization for lithium recovery from high-concentrated aqueous solutions. J. Membr. Sci. 505, 167–173. https://doi.org/10.1016/j.memsci.2016.01.033.

Sorour, M.H., Hani, H.A., Shaalan, H.F., Al-Bazedi, G.A., 2015. Schemes for salt recovery from seawater and RO brines using chemical precipitation. Desal. Water Treat. 55, 2398–2407. https://doi.org/10.1080/19443994.2014.946720.

Sorour, M.H., Hani, H.A., Shaalan, H.F., 2016. Separation of calcium and magnesium using dual precipitation/chelation scheme from saline solutions. Desal. Water Treat. 57, 22818–22823. https://doi.org/10.1080/19443994.2015.1114170.

Silvestroni, 2020. In: Pasquali, M., Latini, A. (Eds.), Fondamenti di Chimica, eleventh ed. CEA.

U.S. Geological Survey, 2017. PHREEQC Version 3. https://www.usgs.gov/software/phreeqc-version-3.

Vavrusova, M., Garcia, A.C., Danielsen, B.P., Skibsted, L.H., 2017. Spontaneous supersaturation of calcium citrate from simultaneous isothermal dissolution of sodium citrate and sparingly soluble calcium hydroxycarboxylates in water. RSC Adv 7, 3078–3088. https://doi.org/10.1039/c6ra25807g.

Wang, W., Hu, M., Zheng, Y., Wang, P., Ma, C., 2011. CO_2 fixation in Ca^{2+}/Mg^{2+} rich aqueous solutions through enhanced carbonate precipitation. Ind. Eng. Chem. Res. 50, 8333–8339. https://doi.org/10.1021/ie1025419.

Wang, Y., Qin, Y., Wang, B., Jin, J., Wang, B., Cui, D., 2020. Selective removal of calcium ions from seawater or desalination brine using a modified sodium carbonate method. Desal. Water Treat. 174, 123–135. https://doi.org/10.5004/dwt.2020.24828.

Zavitsas, A.A., 2005. Aqueous solutions of calcium ions: hydratation numbers and the effect of temperature. J. Phys. Chem. B 109, 20636–20640. https://doi.org/10.1021/jp053909i.

Zhang, Y., Dawe, R.A., 2000. Influence of Mg2+ on the kinetics of calcite precipitation and calcite crystal morphology. Chem. Geol. 163, 129–138.